



THE UNIVERSITY
of EDINBURGH



Cardiac re-entry dynamics in MRI- and micro-CT based models of the heart

Irina V. Biktasheva^{1,2}

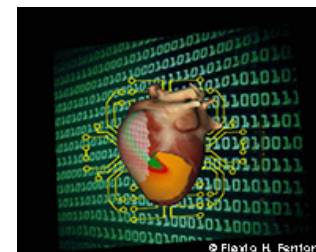
in collaboration with

Richard A. Anderson³, Vadim N. Biktashev², Arun V. Holden⁴, Sanjay R. Kharche^{1,2},
Eleftheria Pervolaraki⁴, Girish Ramlugun⁵, Gunnar Seemann^{6,7},
Bruce Smaill⁵, FenCai Wen¹

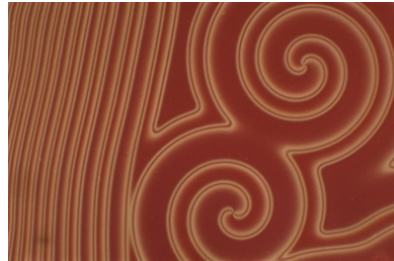
¹ University of Liverpool, UK; ² University of Exeter, UK; ³ University of Edinburgh, UK; ⁴ University of Leeds, UK;

⁵ Auckland Bioengineering Institute, The University of Auckland, New Zealand;

⁶ Karlsruhe Institute of Technology, Germany; ⁷The University Heart Center, Freiburg, Germany.



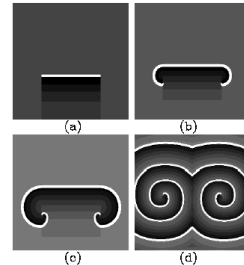
Dissipative vortices



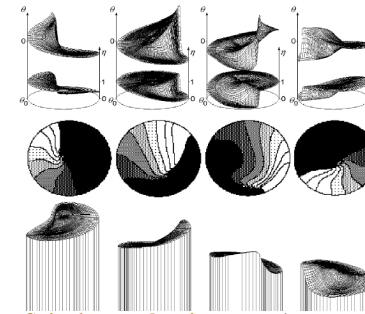
in liquid crystals (S.Residori, Institut Non Linéair de Nice)



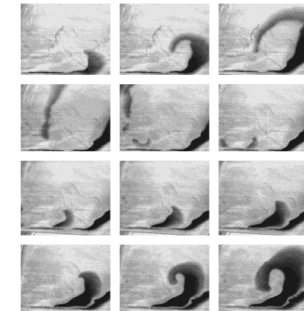
Galaxy M5 (Hubble telescope).



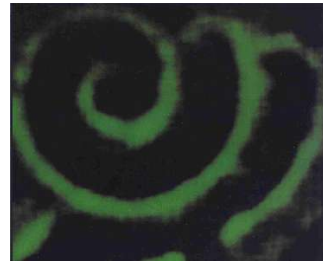
in lasers (numerics: J.Simonotto, Herriot-Watt; experiment: Someone at Lebedev Inst. Moscow?)



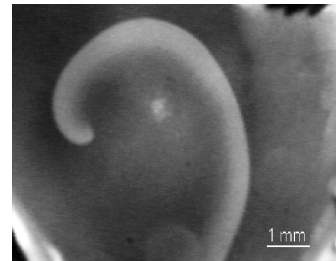
Spinning combustion wave (numerics: A.Merzhanov+T.Ivleva, Chernogolovka)



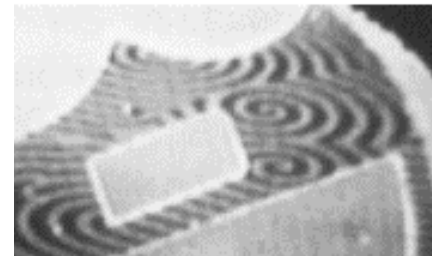
rusting of steel surface in nitric acid (O.Steinbock, Florida)



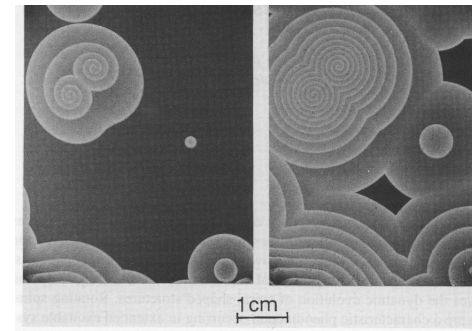
Ca waves in oocytes (D.E.Clapham, Harvard)



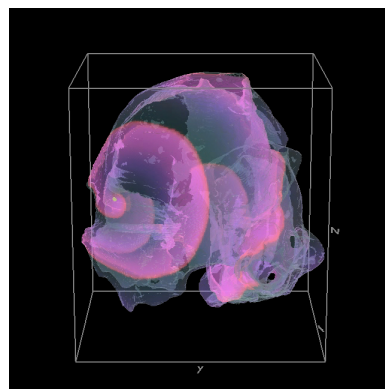
spreading depression in chicken retina (M.A.Dahlem, Magdeburg)



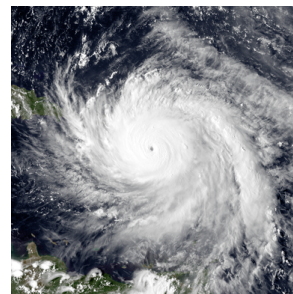
Catalytic CO oxidation on Pt surface (Y.Kevrekidis, Princeton)



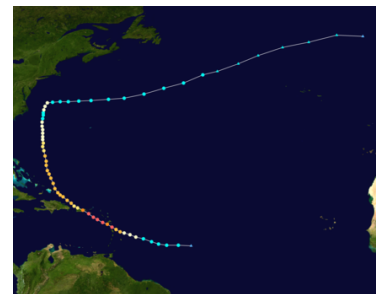
Belousov-Zhabotinsky (BZ) reaction medium (Stefan C.Muller+Theo Plesser)



re-entry of excitation in human atrium

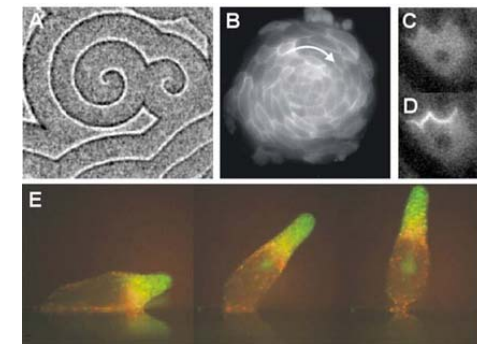


Hurricane Maria near peak intensity NW of Dominica, Sept 19 2017.



Map plotting the track and intensity of the storm, according to the Saffir-Simpson scale

https://en.wikipedia.org/wiki/Hurricane_Maria



in slime moulds (C.Weijer, Dundee)

Unperturbed Dynamics

- Reaction-diffusion system for ℓ components

$$\partial_t \mathbf{u} = \mathbf{f}(\mathbf{u}) + \mathbf{D} \nabla^2 \mathbf{u} + \epsilon \mathbf{h}, \quad \mathbf{u}, \mathbf{f}, \mathbf{h} \in \mathbb{R}^\ell, \quad \mathbf{D} \in \mathbb{R}^{\ell \times \ell}, \quad \ell \geq 2.$$

- Steadily rotating spiral wave solutions ($\epsilon = 0$):

$$\mathbf{u}(\vec{r}, t) = \mathbf{U}(\rho(\vec{r} - \vec{R}), \vartheta(\vec{r} - \vec{R}) + \omega t - \Phi).$$



1D: Front existence (initiation) & dissipation

E.g. V.N. Biktashev and R. Suckley, *Phys. Rev. Lett.*, 93(16):168103, 2004
 I.V. Biktasheva, et. al, *FIMH 2005, LNCS 3504*: 293-303, 2005.

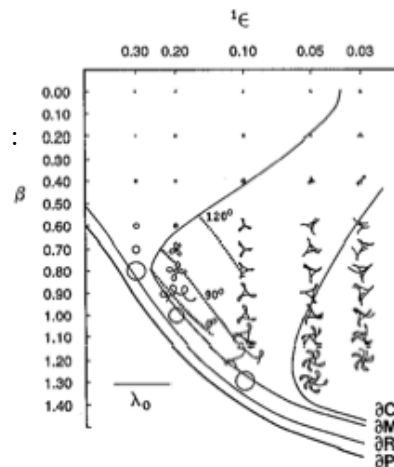
2D: Meander

FitzHugh - Nagumo (FHN) model :

$$\partial_t u_1 = \epsilon^{-1}(u_1 - u_1^3/3 - u_2) + D \nabla^2 u_1,$$

$$\partial_t u_2 = \epsilon(u_1 + \beta - \gamma u_2) + \nabla^2 u_2.$$

A.T. Winfree,
CHAOS, 1(3), 1991 >>



3D: Filament tension (negative)

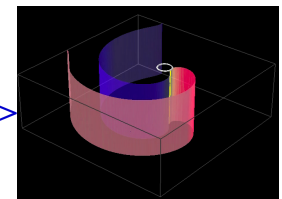
- ✓ Scroll turbulence

V.N. Biktashev, et.al, *PTRSA*, 347: 611-630, 1994
 V.N. Biktashev, *IJBC*, 8(4): 677-684, 1998



- ✓ Buckling

H. Dierckx, et.al, *PRL*, 109(17):174102, 2012 >>



Perturbation theory: the problem

V.N. Biktashev and A.V. Holden, *Chaos, Solitons and Fractals* 5(3,4): 575-622, 1995

- Reaction-diffusion system for ℓ components

$$\partial_t \mathbf{u} = \mathbf{f}(\mathbf{u}) + \mathbf{D} \nabla^2 \mathbf{u} + \epsilon \mathbf{h}, \quad \mathbf{u}, \mathbf{f}, \mathbf{h} \in \mathbb{R}^\ell, \quad \mathbf{D} \in \mathbb{R}^{\ell \times \ell}, \quad \ell \geq 2.$$

- Steadily rotating spiral wave solutions ($\epsilon = 0$):

$$\mathbf{u}(\vec{r}, t) = \mathbf{U}(\rho(\vec{r} - \vec{R}), \vartheta(\vec{r} - \vec{R}) + \omega t - \Phi).$$

($\vec{r} = (x, y)$, $\vec{R} = (X, Y) = \text{const}$, $\Phi = \text{const}$, ω is an eigenvalue).

- For $\epsilon \neq 0$, the spiral drifts: solution remains approximately as above, but $d\vec{R}/dt = \mathcal{O}(\epsilon)$, $d\Phi/dt = \mathcal{O}(\epsilon)$.

E.g.

- **alternanses**

E. Koch, *Pflügers Arch.*, 181: 106, 1920

A. Karma, “Electrical alternans and spiral wave breakup in cardiac tissue”, *Chaos*, 4(3), pp 461-472, 1994.

- **inhomogeneity**

V.N. Biktashev, D. Barkley and I.V. Biktasheva, “Orbital motion of spiral waves in excitable media”, *PRL*, 104(5): 058302, 2010 >>

- **anisotropy**

F. Fenton, A. Karma, “Fiber-rotation-induced vortex turbulence in thick myocardium”, *PRL*, 81(2), pp 481-484, 1998

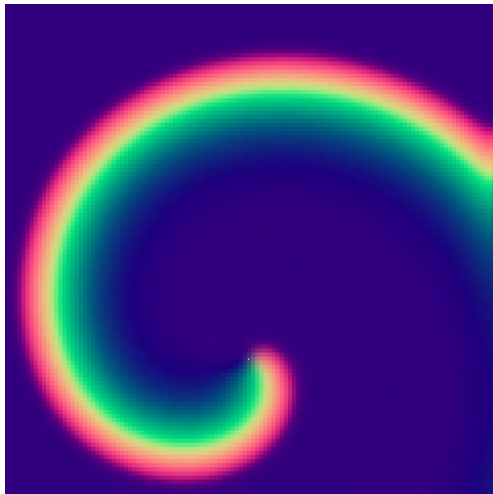
O. Berenfeld, M. Wellner, J. Jalife, A.M. Pertsov, “Shaping of a scroll wave filament by cardiac fibers”, *PRE*, 63(6): 061901, 2001

- **curvature of the domain**

H. Dierckx, E. Brisard, H. Verschelde, A.V. Panfilov, “Drift laws for spiral waves on curved anisotropic surfaces”, *PRE*, 88(1): 012908, 2013



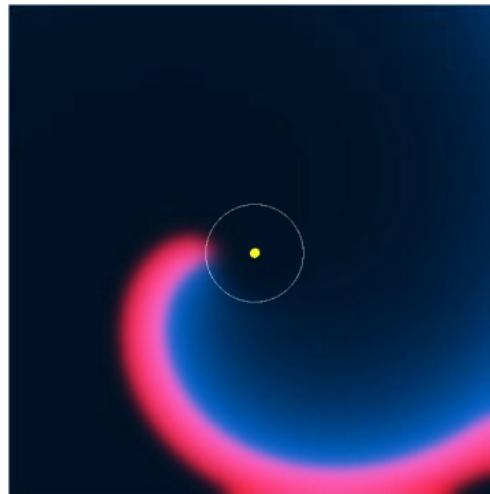
Drift caused by inhomogeneity



- Half of the medium is slightly different than the other.

V.N. Biktashev & A.V. Holden
 ``Resonant drift of autowave vortices in 2D and the effects of boundaries and inhomogeneities'', *Chaos, Solitons and Fractals* 5(3,4): 575-622, 1995

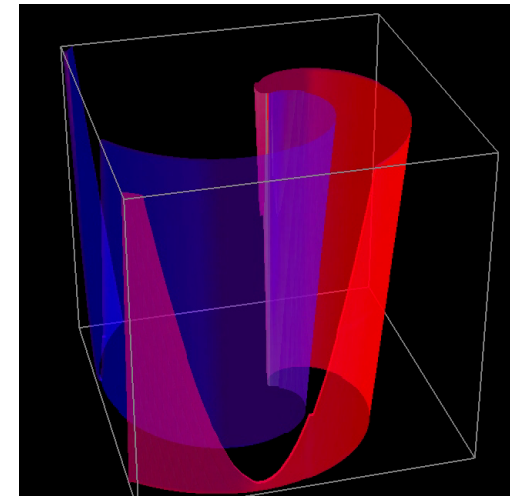
I.V. Biktasheva, "Drift of spiral waves in the Complex Ginzburg-Landau Equation due to media inhomogeneities", *Phys. Rev. E*, 62(6):8800-8803, 2000



- Orbital motion around localized inhomogeneity
- Here, the spiral is kept at a stable distance, which depends on the RFs (i.e. medium parameters) not inhomogeneity strength!

V.N. Biktashev, D. Barkley and I.V. Biktasheva ``Orbital motion of spiral waves in excitable media" *Phys. Rev. Lett.*, **104**(5): 058302, 2010

Scroll turbulence at negative filament tension



- Filament equation of motion:

$$(\vec{N} + i\vec{B}) \cdot \vec{R} = (b_2 + ic_3)\kappa$$

where b_2 is filament tension.

Total length:

$$\frac{d}{dt} \int ds = - \int b_2 \kappa^2 ds + \text{bound. eff.}$$

V.N. Biktashev, A.V. Holden & H. Zhang, ``Tension of Organizing Filaments of Scroll Waves" *Phil. Trans. Roy. Soc. London, ser A* **347**: 611-630, 1994

V.N. Biktashev ``A Three-Dimensional Autowave Turbulence" *Int. J. Bifurcation & Chaos*, **8**(4): 677-684, 1998

Macroscopic Dissipative Wave-Particle Duality

A popular introduction by Dwight Barkley



http://www.youtube.com/watch?v=YGVVZVD_ddd

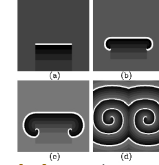
- **Localization** of the adjoint symmetry modes, aka the **Response Functions (RFs)**, means that spiral waves behave like point objects, and scroll waves behave like string objects.
- **The asymptotic theory** based on the RFs
 - is (within its limits) in good quantitative agreement with direct simulations.
 - **predicted new qualitative phenomena:**
 - orbital motion,
 - pinning to repelling inhomogeneity,
 - interaction with small variation of thickness in a layer, etc.



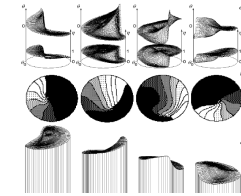
in liquid crystals
(S.Residori,
Institut Non Linéair
de Nice)



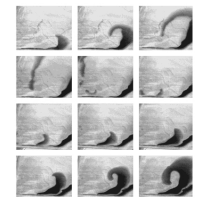
*Galaxy M5 (Hubble
telescope).*



in lasers (numerics:
J.Simonotto,
Herriot-Watt;
experiment:
Someone at Lebedev
Inst. Moscow?)



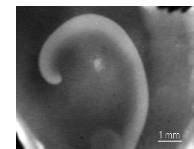
Spinning combustion wave
(numerics: A.Merzhano
v+T.Ivleva, Chernogolovka)



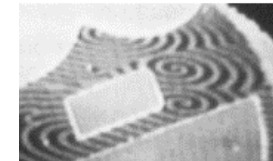
**rusting of steel surface
in nitric acid**
(O.Steinbock, Florida)



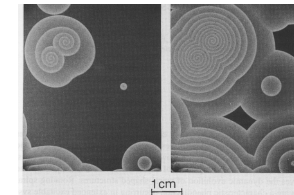
Ca waves in oocytes
(D.E.Clapham, Harvard)



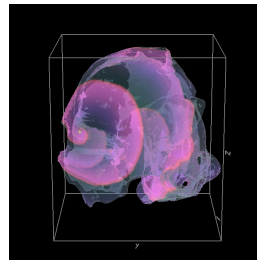
**spreading depression
in chicken retina**
(M.A.Dahlem,
Magdeburg)



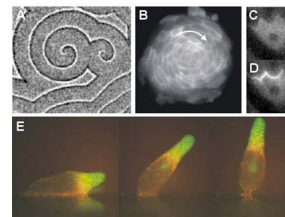
**Catalytic CO oxidation
on Pt surface**
(Y.Kevrekidis, Princeton)



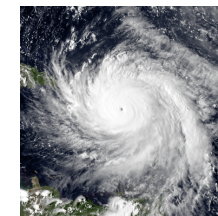
**Belousov-Zhabotinsky (BZ)
reaction medium**
(Stefan C.Muller+Theo Plesser)



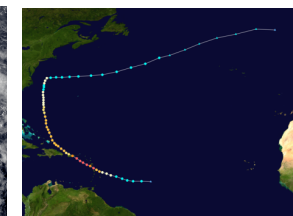
**re-entry of excitation
in human atrium**



in slime moulds (C.Weijer,
Dundee)



Hurricane Maria near peak
intensity NW of Dominica,
Sept 19 2017.



Map plotting the track and
intensity of the storm, according
to the Saffir-Simpson scale

https://en.wikipedia.org/wiki/Hurricane_Maria

I.V. Biktasheva, V.N. Biktashev, "Wave-particle dualism of spiral waves dynamics", *Phys Rev E*, 67: 026221, 2003

Perturbation theory: result

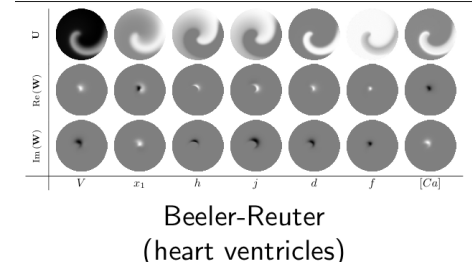
- Drift velocity due to perturbation:

$$\dot{R} = \epsilon \int_{\phi-\pi}^{\phi+\pi} e^{-i\xi} \langle \mathbf{w}, \tilde{\mathbf{h}}(\mathbf{U}; \rho, \theta, \xi) \rangle \frac{d\xi}{2\pi} + \mathcal{O}(\epsilon^2),$$

where (ρ, θ) are corotating polar coordinates and ϕ and ξ measure the rotation phase, $\phi = \omega t - \Phi(t)$, and inner product

$$\langle \mathbf{w}, \mathbf{v} \rangle = \int_{\mathbb{R}^2} \mathbf{w}^+(\vec{r}) \mathbf{v}(\vec{r}) d^2\vec{r} = \oint_0^\infty \int_0^\infty \mathbf{w}^+(\rho, \theta) \mathbf{v}(\rho, \theta) \rho d\rho d\theta.$$

- (Translational) response function $\mathbf{W}(\rho, \theta) \in \mathbb{C}$: eigenfunction of the adjoint linearized operator, corresponding to eigenvalue $i\omega$.



V.N. Biktashev and A.V. Holden, *Chaos, Solitons and Fractals* 5(3,4): 575-622, 1995

V.N. Biktashev, I.V. Biktasheva, and N.A. Sarvazyan, *PLoS ONE*, 6(9):e24388, 2011

Superposition principle

Superposition of various perturbation

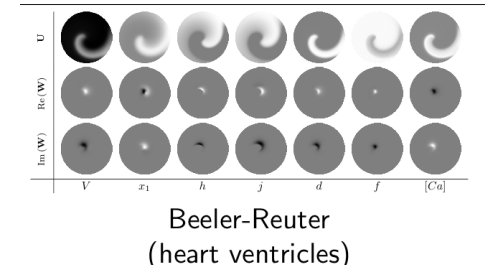
$$\epsilon \mathbf{h} = \sum_j \epsilon_j \mathbf{h}_j,$$

has summative effect on the drift velocity

$$\dot{R} \approx \sum_j \epsilon_j \gamma_j,$$

where “specific forces” are

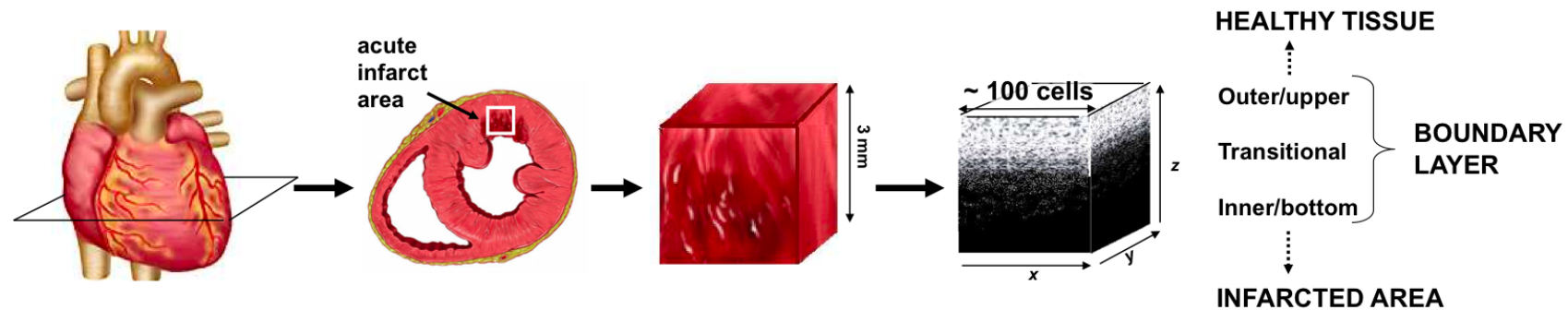
$$\gamma_j = \oint e^{-i\xi} \langle \mathbf{w}, \tilde{\mathbf{h}}_j \rangle \frac{d\xi}{2\pi}.$$



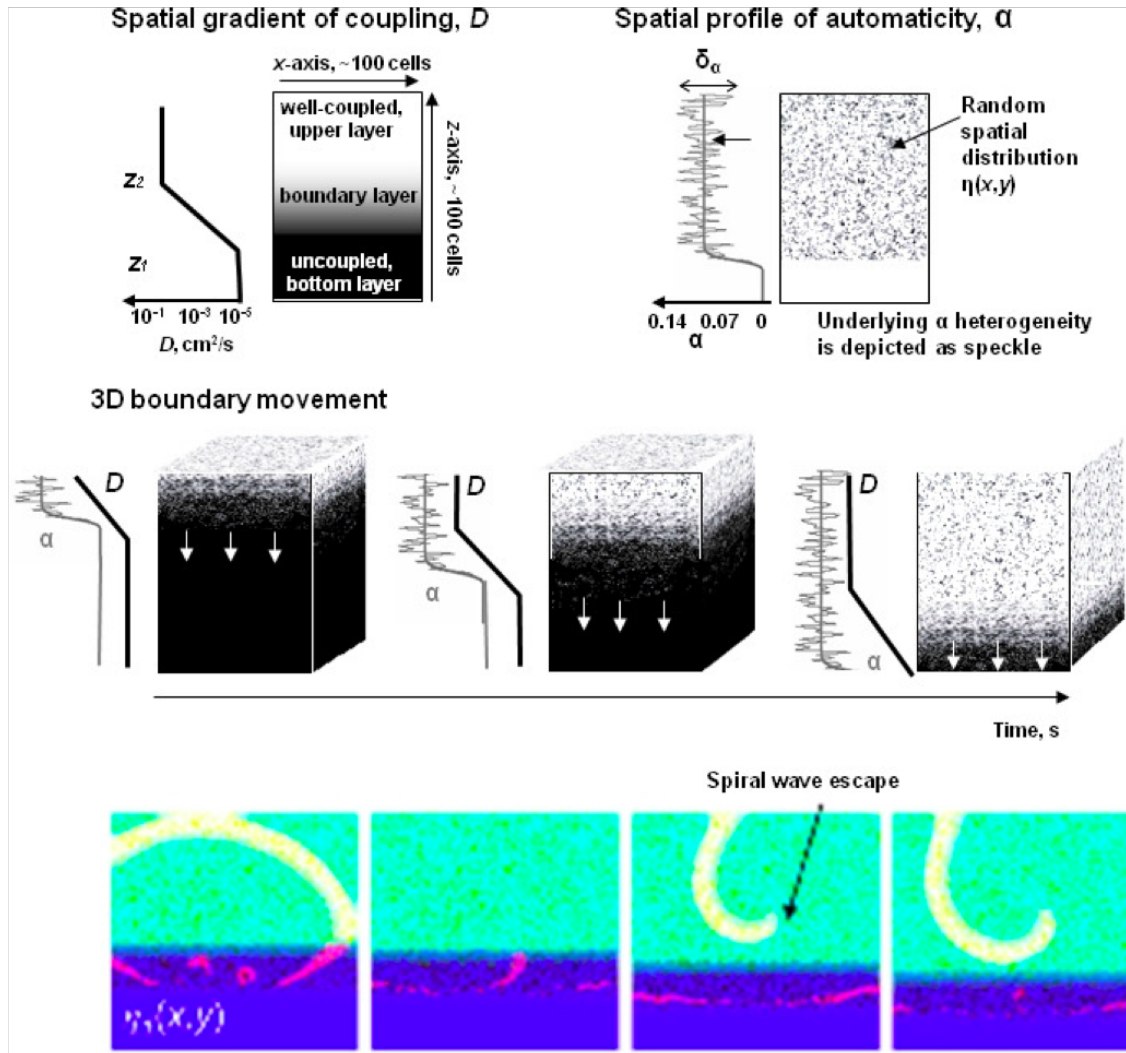
Spiral waves generated near recovering ischaemic boundary: cell culture experiment



V.N. Biktashev, A Arutunyan and N.A. Sarvazyan
"Generation and escape of local waves from the boundary of uncoupled cardiac tissue" *Biophys. J.*, **94**: 3726-3738, 2008



Ischaemic boundary specific forces



γ_D - force of gradient of diffusivity
(= connectivity)

γ_α - force of gradient of excitability α

F - force caused by a localized inhomogeneity of α

γ_K - force due to filament curvature K

$$\gamma_K = b_2 + ic_3$$

where

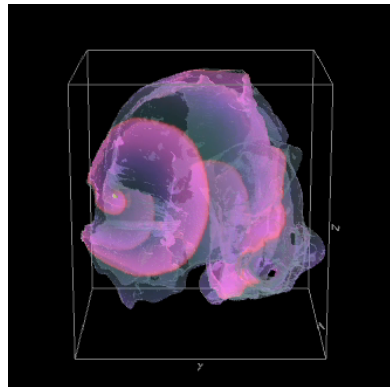
b_2 - filament tension

c_3 - binormal drift coefficient of the filament

NB. $\gamma_D = -\gamma_K$

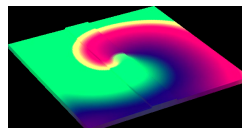
Drift due to variation of thickness of the layer.

Epicardial View



- Ridge --- the CT and PM (attached to wall) ridge structures

Up >>

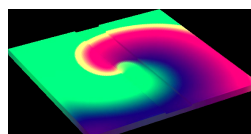


Down >>

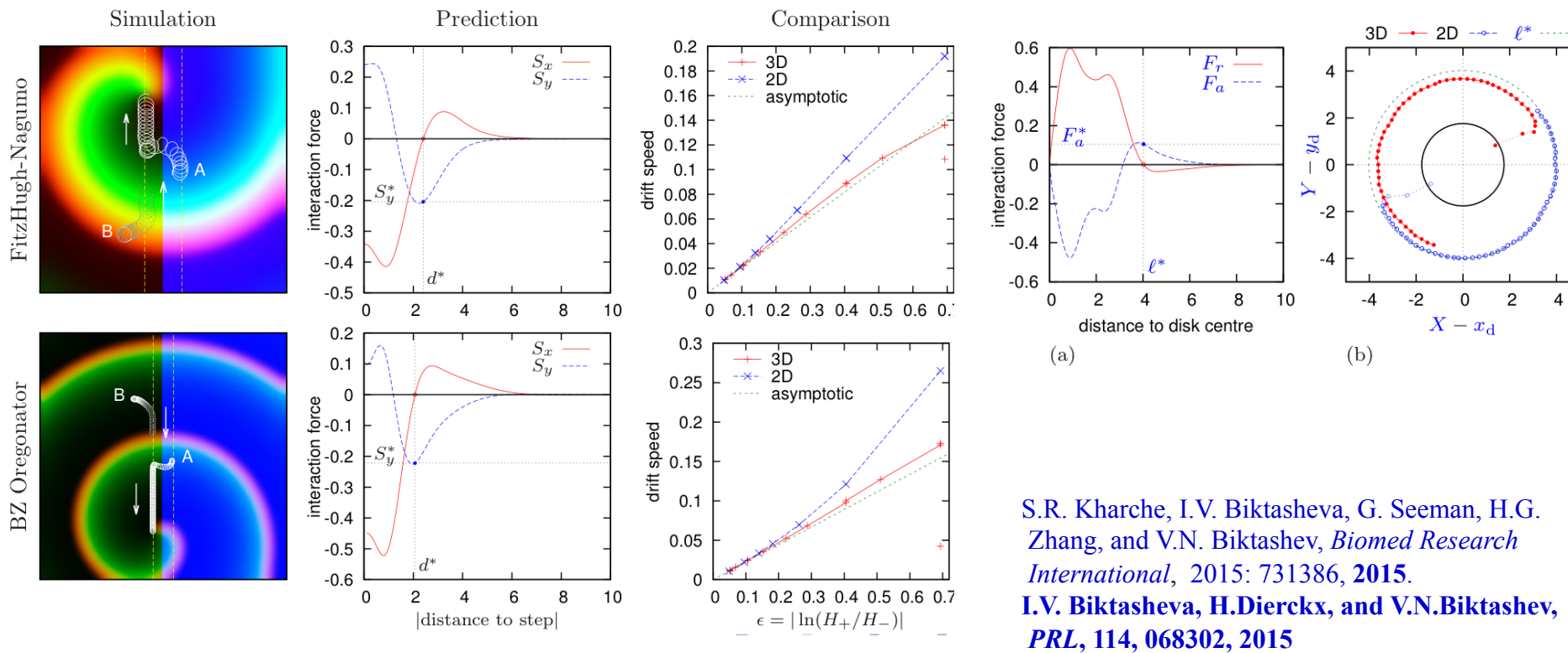
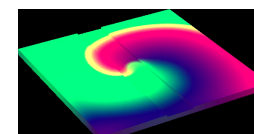


- Ditch --- in between PM (attached to wall) ridge structures

Up >>



Down >>

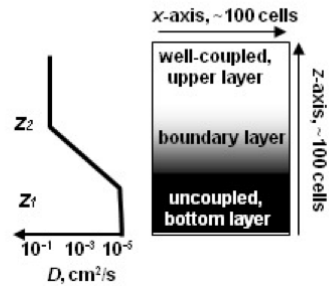


S.R. Kharche, I.V. Biktasheva, G. Seeman, H.G. Zhang, and V.N. Biktashev, *Biomed Research International*, 2015: 731386, 2015.

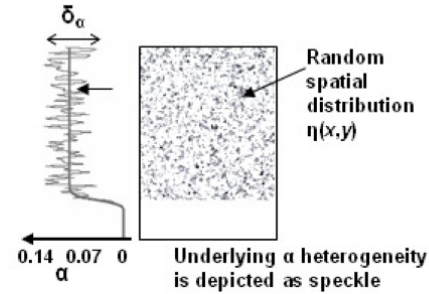
I.V. Biktasheva, H.Dierckx, and V.N.Biktashev, *PRL*, 114, 068302, 2015

specific forces

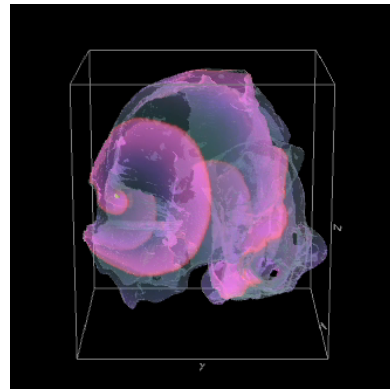
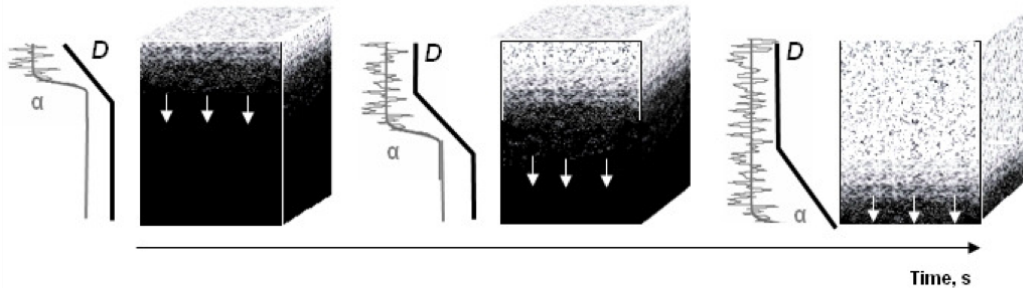
Spatial gradient of coupling, D



Spatial profile of automaticity, α



3D boundary movement



✓ Inhomogeneity

γ_D - gradient of diffusivity (= coupling)

γ_α - gradient of excitability α

F - localized inhomogeneity of α

✓ γ_K - Filament curvature K

$$\gamma_K = b_2 + ic_3$$

where b_2 - filament tension

c_3 - binormal drift velocity

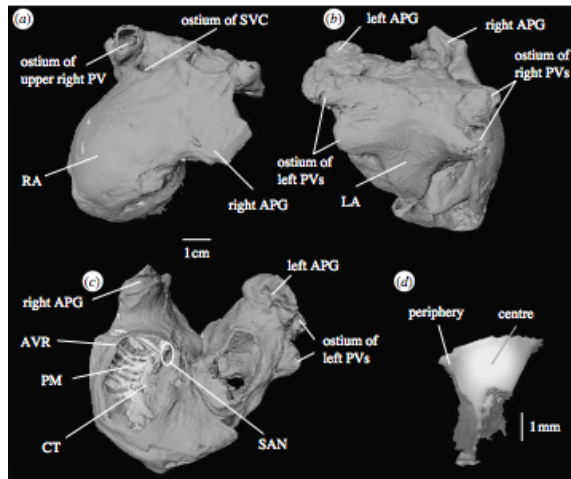
NB. $\gamma_D = -\gamma_K$

✓ Anatomy

- Anisotropy
- Thickness gradients & fluctuations
- Curvature of the Domain

Anatomy Models

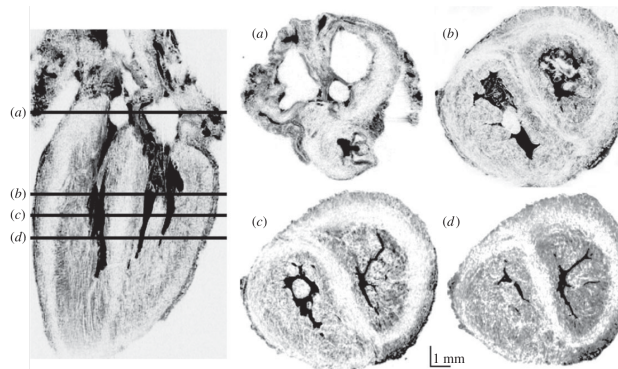
Human Atrium



The model derived from the Visible Female dataset: the transversal cryosections with a resolution of 0.33 mm, and an algorithm for fiber orientation .

G. Seemann, C. Höper, F. B. Sachse, O. Dössel, A. V. Holden, and H. Zhang. Heterogeneous three-dimensional anatomical and electrophysiological model of human atria. In *Phil. Trans. Roy. Soc. A*, vol. 364(1843) , pp. 1465-1481, 2006

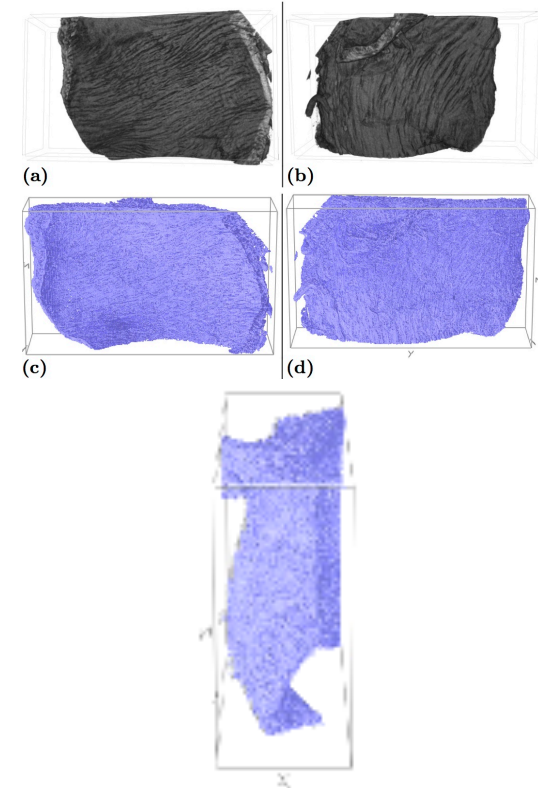
Human Foetal Heart



Fast low- angle shot and diffusion tensor magnetic resonance imaging (DT-MRI) of 139 days of gestation age (DGA) foetal heart, with the voxel resolution of 0.1 mm.

E Pervolaraki, RA Anderson, AP Benson, B Hays-Gill, AV Holden, BJR Moore, MN Paley, HG Zhang, “Antenatal architecture and activity of the human heart”, *INTERFACE FOCUS*, v. 3(2), 20120065, 2013.

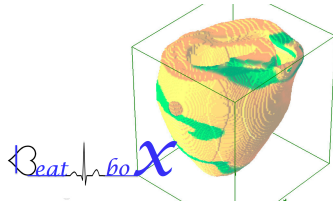
Rat Pulmonary Vein Wall



Micro_CT resolution 3.5 microns in each plane.

[G.S. Ramlugun, B.H. Smaill, unpublished.]

G.S. Ramlugun, B. Thomas, V.N. Biktashev, I.J. LeGrice, B.H. Smaill, J.C. Zhao, and I.V. Biktasheva, "Comparative in-silico study of cardiac re-entry dynamics in micro-CT based models of mammalian hearts", *submitted to Frontiers Physiology*, 2018.



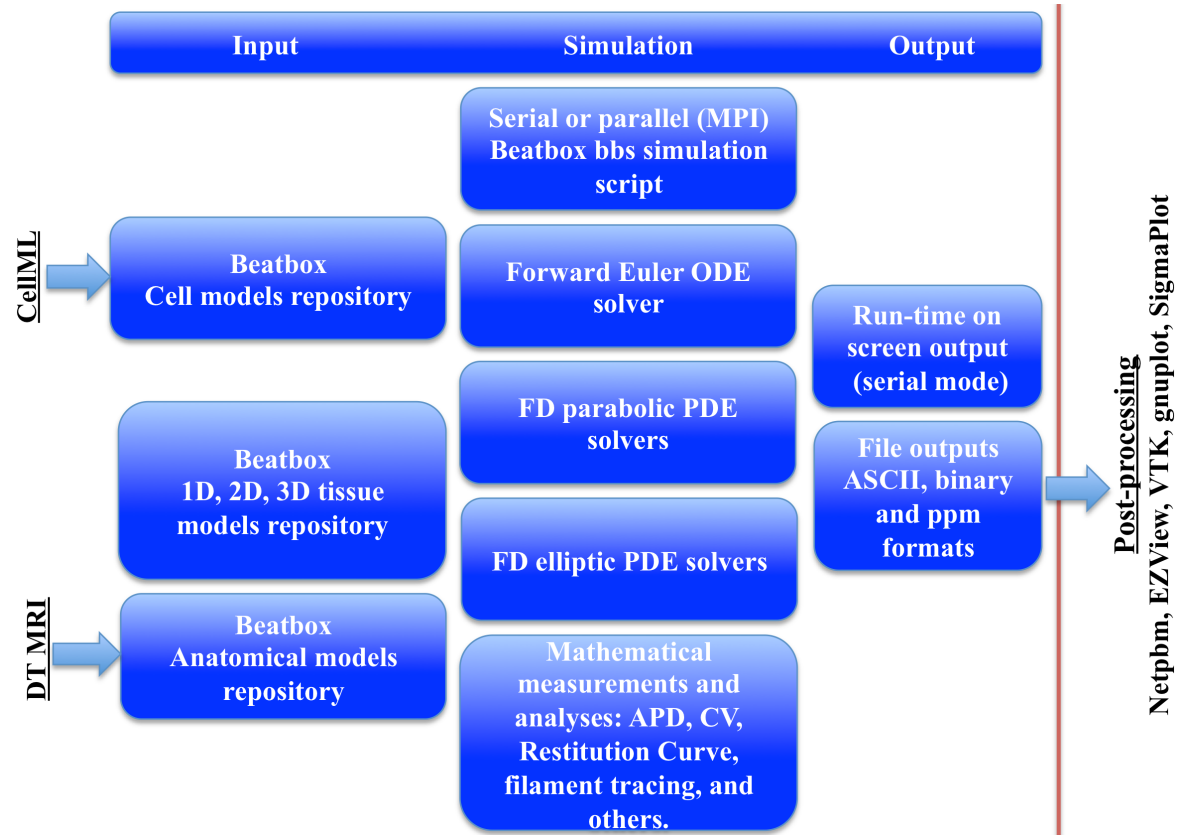
BeatBox Virtual Heart.

✓ **software package following the modular philosophy,** with built-in extendable repository of anatomical and cell models.

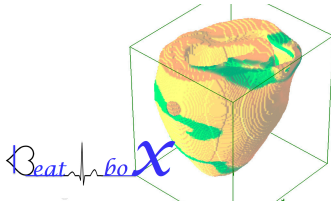
✓ **built in script interpreter** to allow combinatorial flexibility to change from one model to another, without re-compilation of the whole system.

✓ **High Performance Computing:**

“**BeatBox** – HPC Environment for Biophysically and Anatomically Realistic Cardiac Simulations”



M. Antonioletti, V.N. Biktashev, A. Jackson, S.R. Kharche, T. Stary, I.V. Biktasheva, “BeatBox—HPC simulation environment for biophysically and anatomically realistic cardiac electrophysiology”. PLoS ONE 12(5): e0172292, 2017.



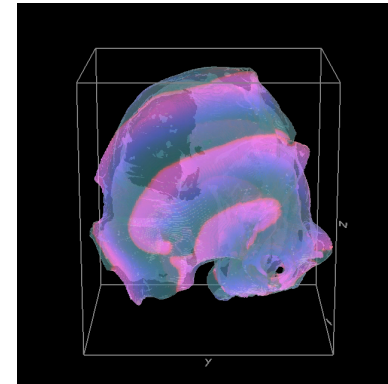
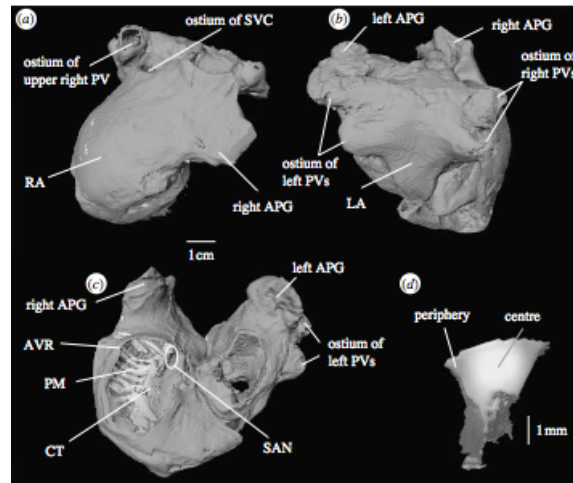
A sample BeatBox script

```
<fhn.par> // model pars are read in from file fhn.par
state geometry=ffr.bbg // file ffr.bbg describes the tissue geometry
def real T; def real begin; def real out; def real end; // real vars control works of “devices”

// The computation
diff v0=[u] v1=[i] Dpar=D Dtrans=D/4 hx=hx; // anisotropic diffusion
k_func when=force pgm={u[i]=u[i]+force};
euler v0=[u] v1=[v] ht=ht ode=fhncubpar={eps=eps bet=@[b] gam=gam lu=@[i]};

// Output
ppmout when=out file="[0]/%04d.ppm" mode="w" // every “out” timesteps
record when=end file=[0].rec when=end v0=0 v1=1; // ascii dump in the end of run
stop when=end;
end;
```

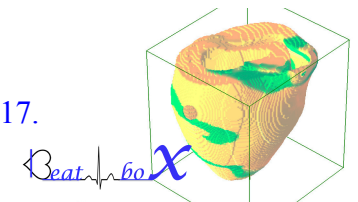
Excitation Re-entry in Human Atrium*



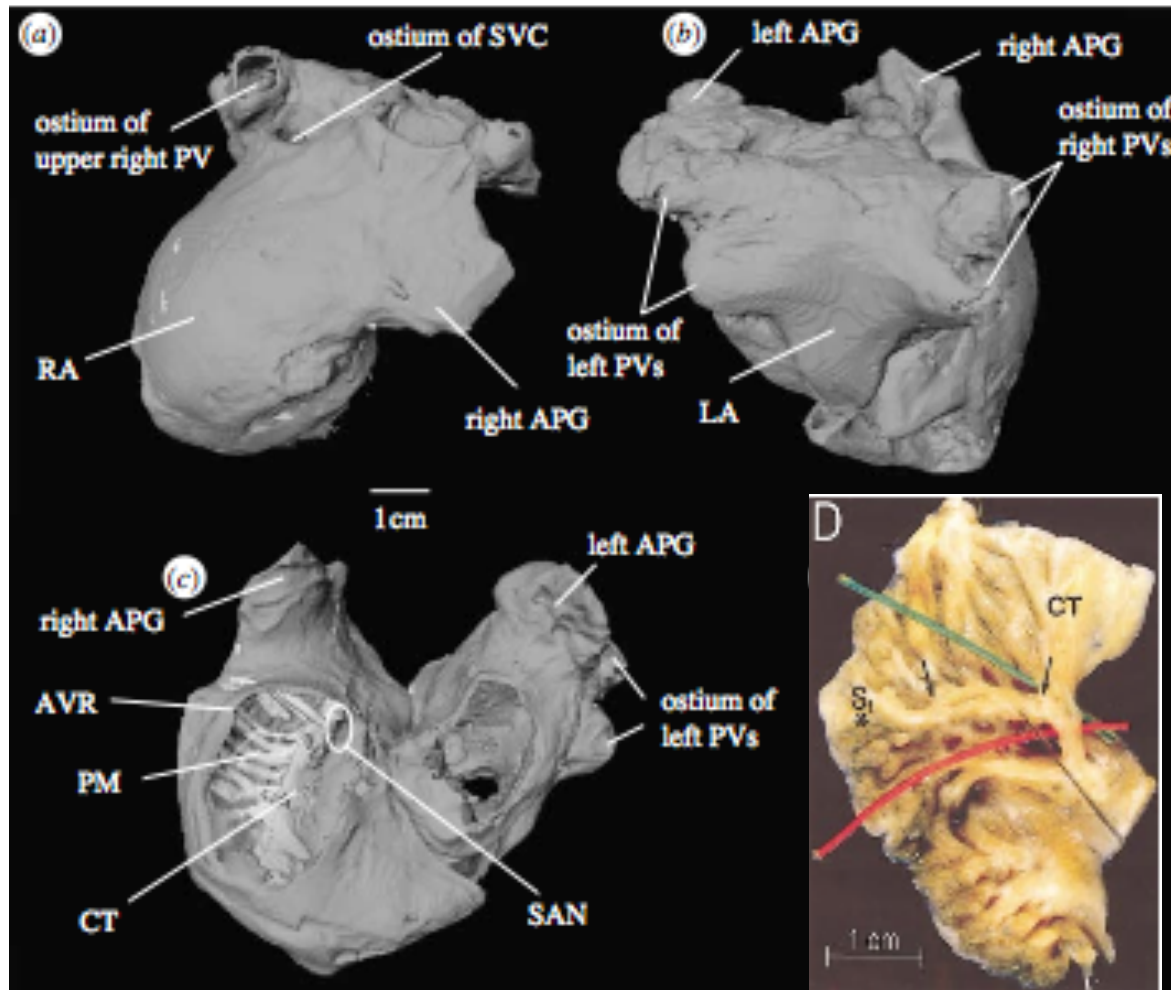
- Regular Cartesian coordinates (cryosections + algorithm fibers):
box of 237x271x300 points, $\Delta x=0.33\text{mm}$
- Explicit Euler in time
- Second order approximation of Laplacian
- Neumann boundary conditions: $1 < \text{approximation order} \leq 2$ **
- Spiral wave initiation by phase distribution
- MPI HPC

•G. Seemann, C. Höper, F. B. Sachse, O. Dössel, A. V. Holden, and H. Zhang. Heterogeneous three-dimensional anatomical and electrophysiological model of human atria. In *Phil. Trans. Roy. Soc. A*, vol. 364(1843), pp. 1465-1481, 2006

** M. Antonioletti, V.N. Biktashev, A. Jackson, S.R. Kharche, T. Stary, I.V. Biktasheva, “BeatBox—HPC simulation environment for biophysically and anatomically realistic cardiac electrophysiology”. *PLoS ONE* 12(5): e0172292, 2017.



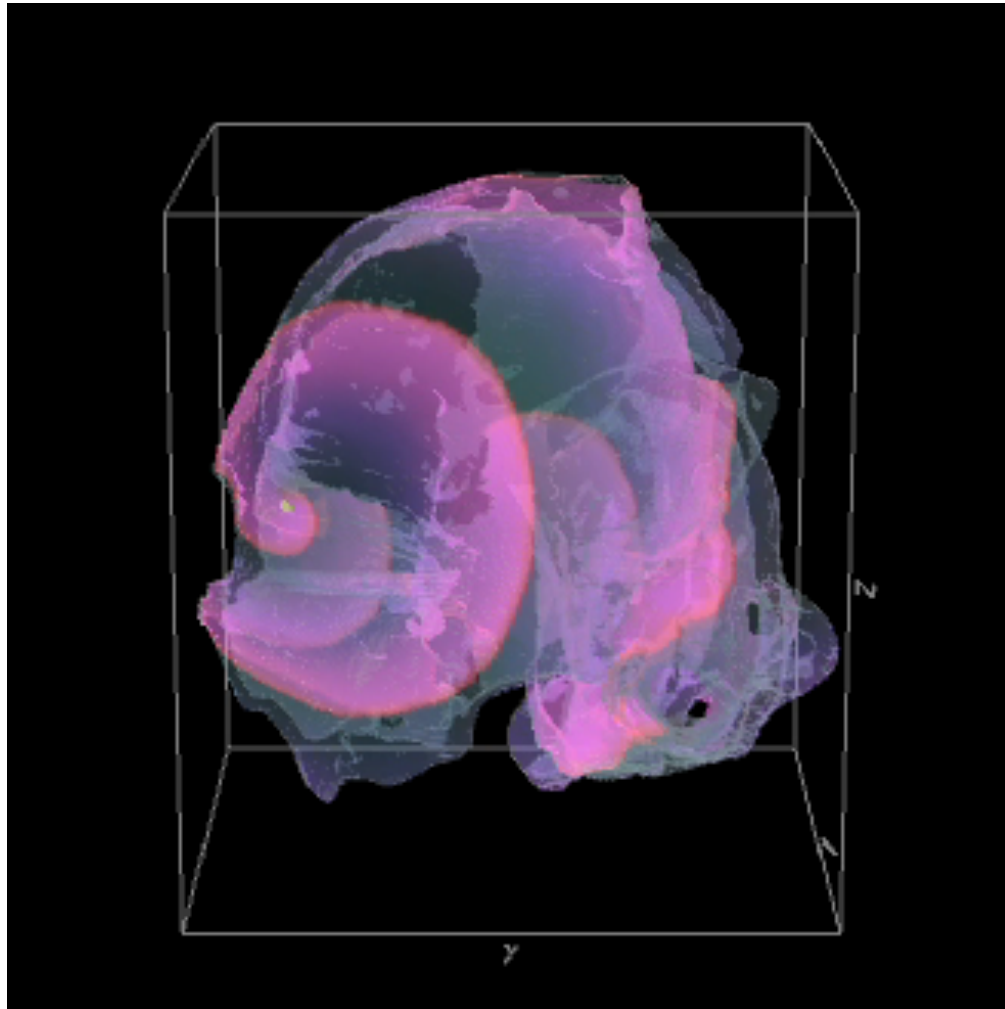
Atrium



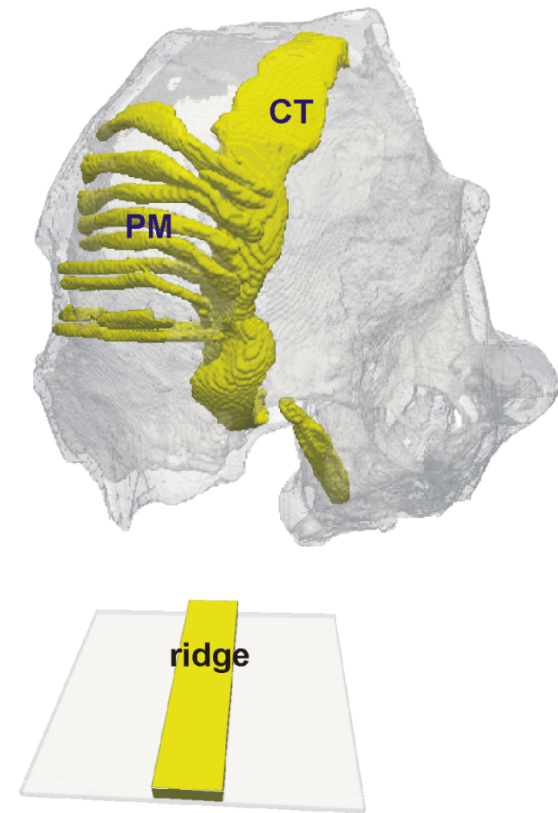
Wu T et al. *Circulation Research*.
1998;83:448-462

G. Seemann, C. Höper, F. B. Sachse, O. Dössel, A. V. Holden, and H. Zhang. Heterogeneous three-dimensional anatomical and electrophysiological model of human atria. In *Phil. Trans. Roy. Soc. A*, vol. 364(1843), pp. 1465-1481, 2006

Anatomy induced drift in Human Atrium



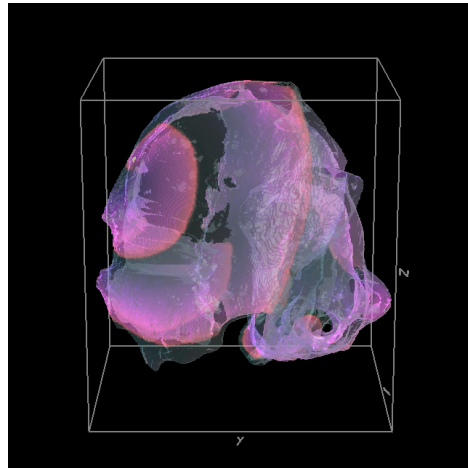
Epicardial View



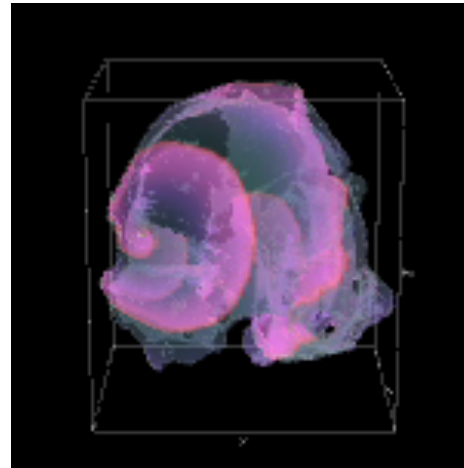
- *Ridge* --- the CT and PM (attached to wall) ridge structures

Anatomy induced drift in Human Atrium

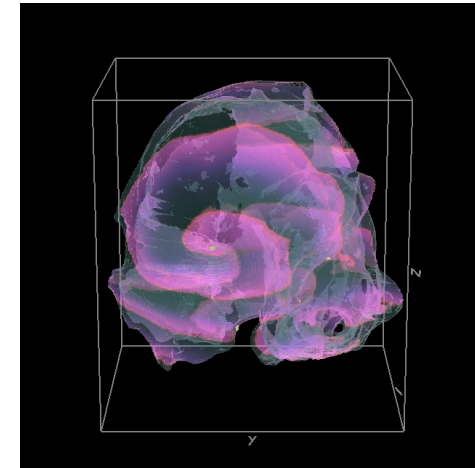
CRN model



Isotropic, $z_0=0.75 \times z_{\max}$, $y_0=0.8 \times y_{\max}$

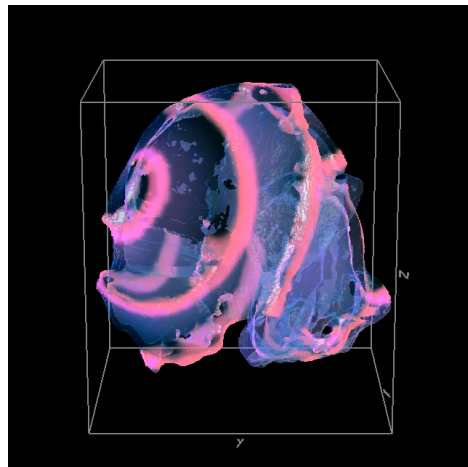


Isotropic, $z_0=0.6 \times z_{\max}$, $y_0=0.8 \times y_{\max}$

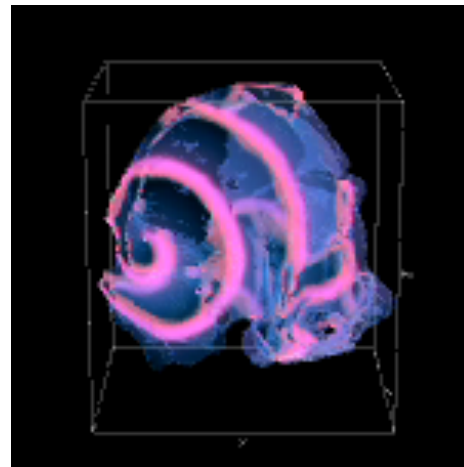


Anisotropic, $z_0=0.6 \times z_{\max}$ $y_0=0.8 \times y_{\max}$
... work in progress...

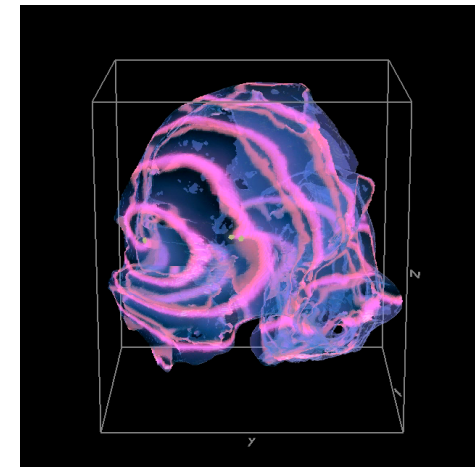
FHN model
($\varepsilon=0.3$; $\beta=0.71$; $\gamma=0.5$)



Isotropic, $z_0=0.75 \times z_{\max}$, $y_0=0.8 \times y_{\max}$

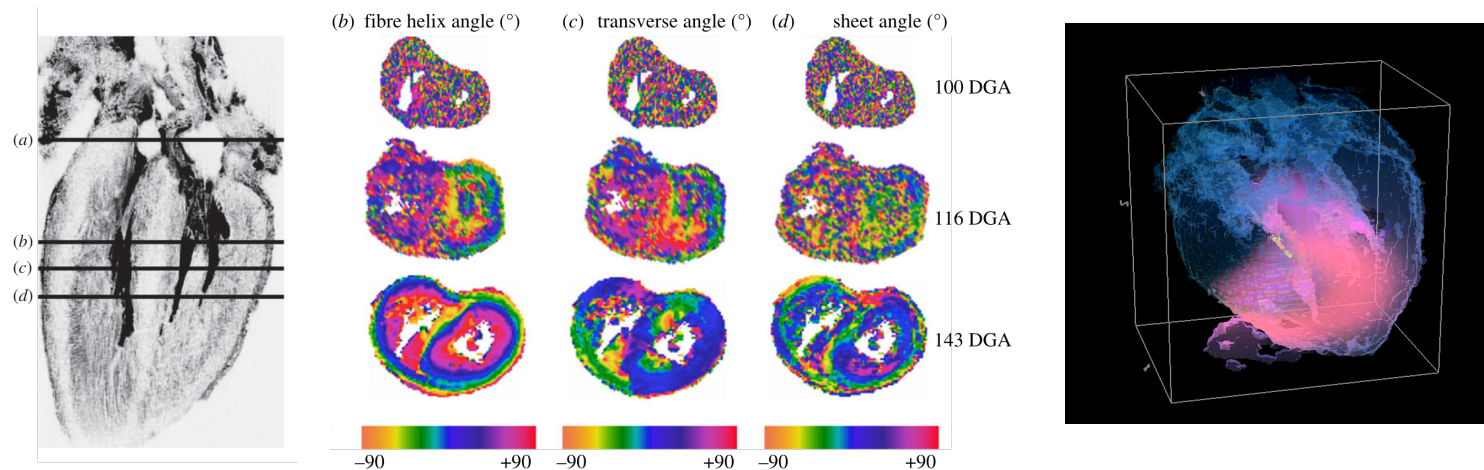


Isotropic, $z_0=0.6 \times z_{\max}$, $y_0=0.8 \times y_{\max}$



Anisotropic, $z_0=0.6 \times z_{\max}$ $y_0=0.8 \times y_{\max}$

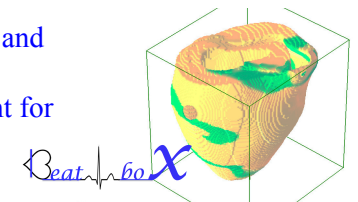
Excitation Re-entry in Foetal Heart *



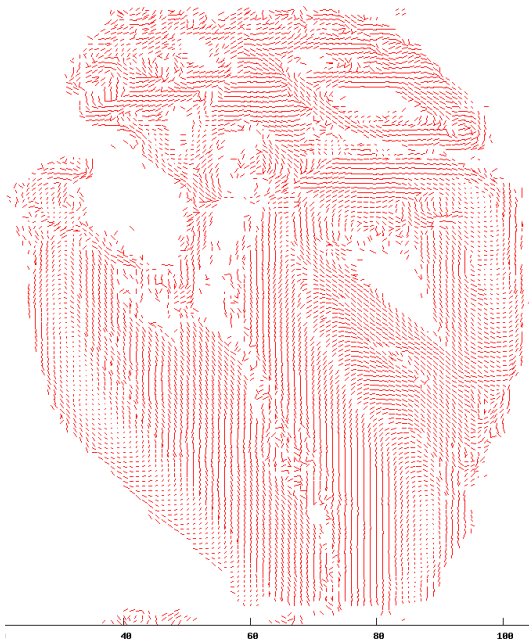
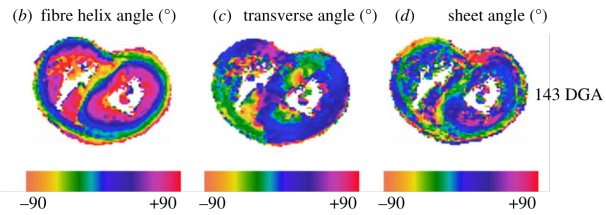
- Regular Cartesian coordinates (DT-MRI):
box of 128 x 128 x 128 points, $\Delta x=0.1\text{mm}$;
- Explicit Euler in time
- Second order approximation of Laplacian
- Neumann boundary conditions: $1 < \text{approximation order} \leq 2$ **
- FHN model: $\varepsilon=0.3$; $\beta=0.71$; $\gamma=0.5$ (rigid rotation, positive filament tension)
- Spiral wave initiation by phase distribution
- MPI HPC

• E Pervolaraki, RA Anderson, AP Benson, B Hays-Gill, AV Holden, BJR Moore, MN Paley, HG Zhang, “Antenatal architecture and activity of the human heart”, *INTERFACE FOCUS*, v. 3(2), 20120065, 2013.

** M. Antonioletti, V.N. Biktashev, A. Jackson, S.R. Kharche, T. Stary, I.V. Biktasheva, “BeatBox—HPC simulation environment for biophysically and anatomically realistic cardiac electrophysiology”. *PLoS ONE* 12(5): e0172292, 2017.

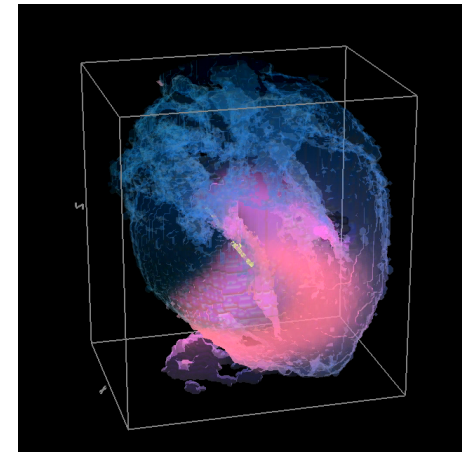


Role of anisotropy in cardiac re-entry dynamics & self-termination.



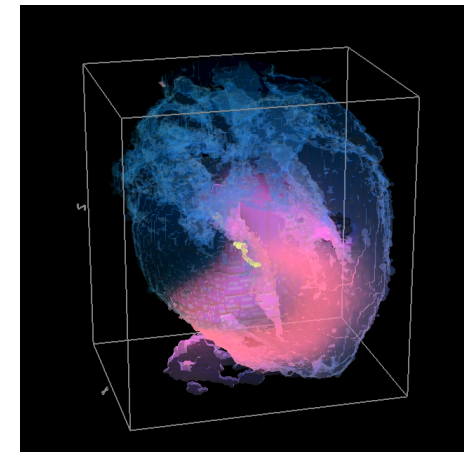
Formed laminar intramural fibres vs chaotic outer-wall regions*

a) Isotropic conduction: 2D – pinning ;



3D – persistent re-entry;

b) AnIsotropic conduction: 2D – persistent re-entry;



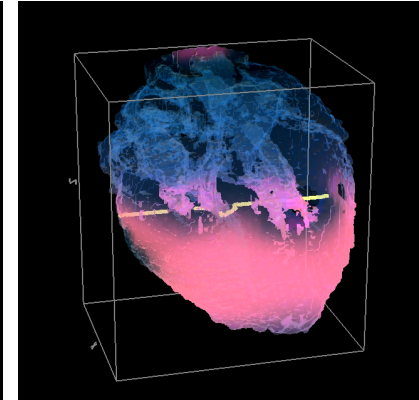
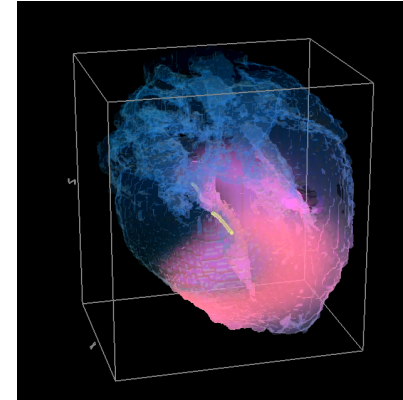
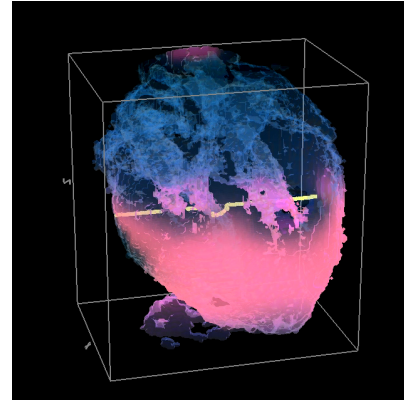
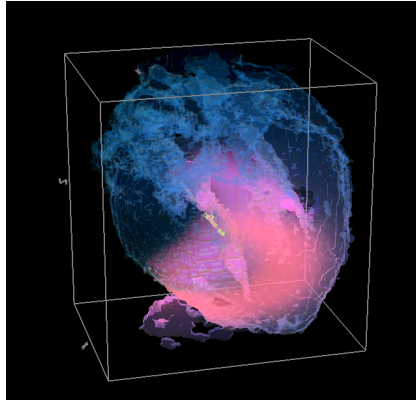
3D – self-termination;

Role of anisotropy in cardiac re-entry dynamics & self-termination.

Original MRI

“Edited” MRI

Isotropic



**Termination
time (a.u.)**

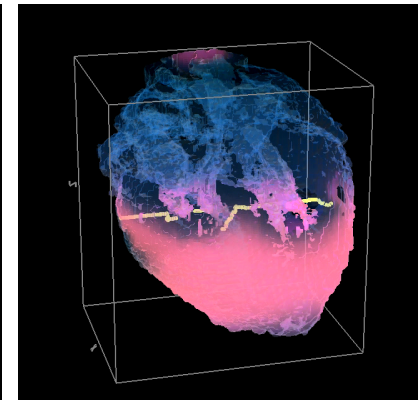
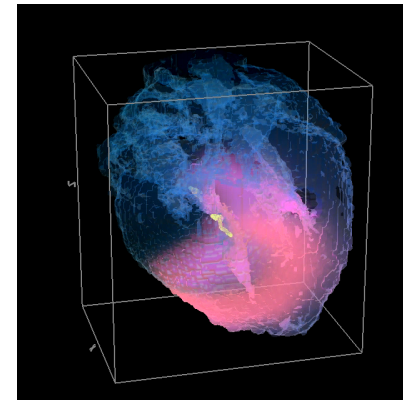
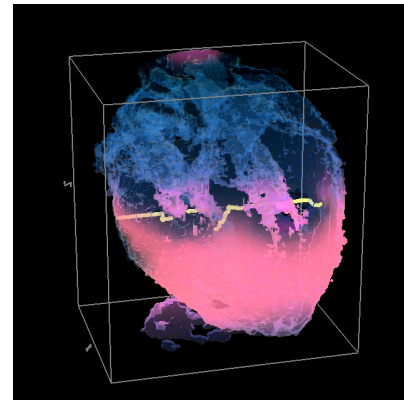
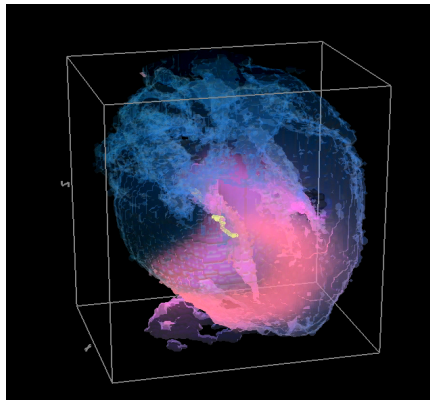
$t = \infty$

$t = 75$

$t = 175$

$t = 75$

AnIsotropic



**Termination
time (a.u.)**

$t = 100$

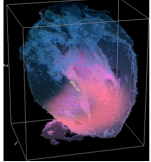
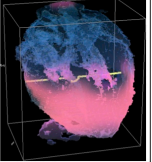
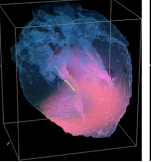
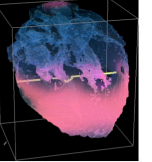
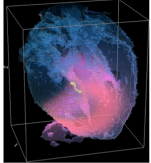
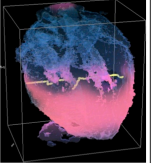
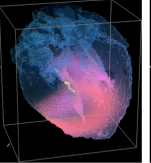
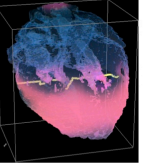
$t = 40$

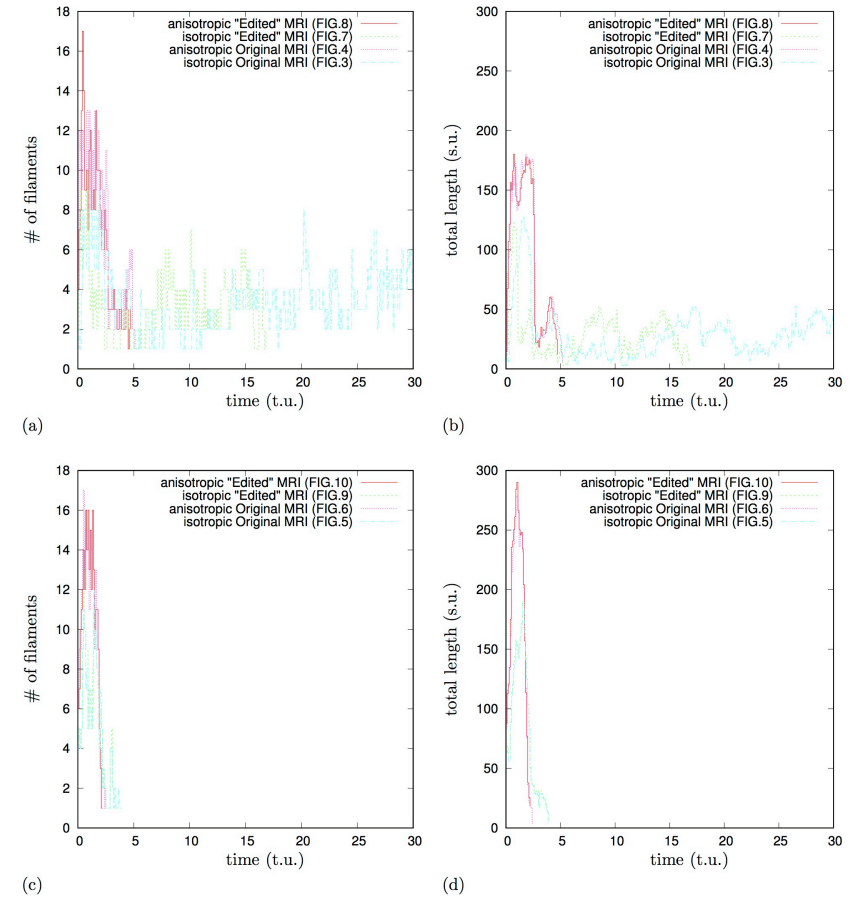
$t = 60$

$t = 30$

I.V. Biktasheva, R.A. Anderson, A.V. Holden, E. Pervolaraki, and F.C. Wen, "Cardiac re-entry dynamics & self-termination in DT-MRI based model of Human Foetal Heart", *Frontiers Phys.* 6:15, 2018

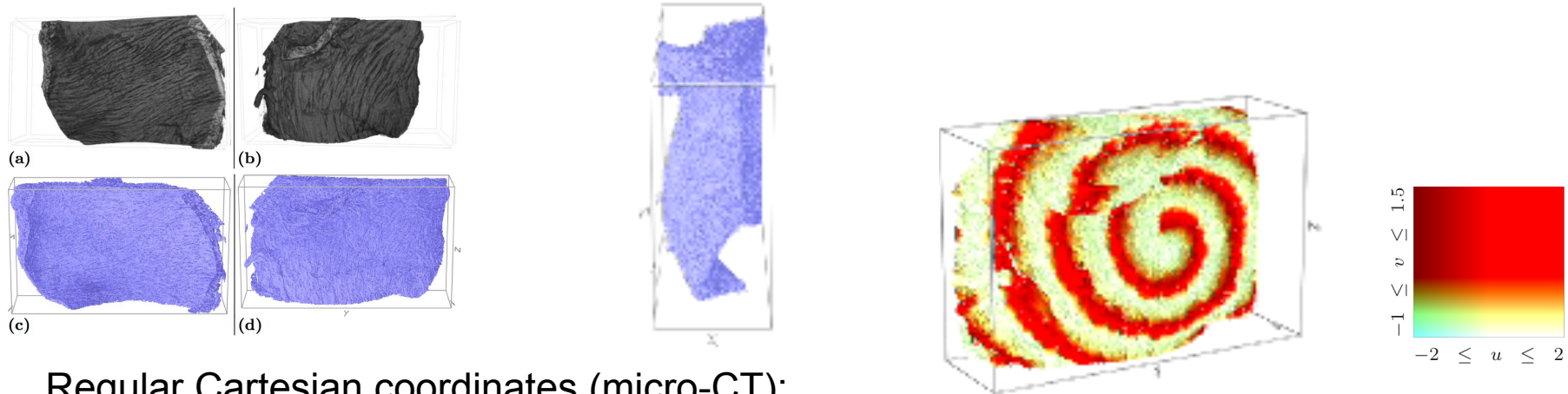
Role of anisotropy in cardiac re-entry dynamics & self-termination.

	Original MRI		"Edited" MRI	
Isotropic				
Simulation FIG.	FIG.3	FIG.5	FIG.7	FIG.9
Filaments Termination time (t.u)	$t=\infty$	t=4.0	t=16.9	t=4.0
Recovery time (t.u)	$t=\infty$	t=7.5	t=17.5	t=7.5
Average # of filaments	3.4	4.7	3.2	4.7
Average total length	29.3	80.5	28.7	82.9
$max(\# \text{ of filaments})(t_{max(\# \text{ of filaments})})$	9 (t=1.0)	12 (t=1.4)	9 (t=0.2)	12 (t=0.5)
$max(\text{total length})(t_{max(\text{total length})})$	127.1 (t=1.6)	188.0 (t=1.5)	122.3 (t=0.7)	190.7 (t=1.5)
AnIsotropic				
Simulation FIG.	FIG.4	FIG.6	FIG.8	FIG.10
Filaments Termination time (t.u)	t=5.3	t=2.6	t=4.8	t=2.3
Recovery time (t.u)	t=10.0	t=4.0	t=6.0	t=3.0
Average # of filaments	6.5	9.5	6.3	10.3
Average total length	91.2	152.6	95.4	177.0
$max(\# \text{ of filaments})(t_{max(\# \text{ of filaments})})$	13 (t=0.8)	17 (t=0.5)	17 (t=0.4)	16 (t=0.7)
$max(\text{total length})(t_{max(\text{total length})})$	179.7 (t=1.8)	278.6 (t=0.9)	180.3 (t=0.7)	290.2 (t=1.0)



I.V. Biktasheva, R.A. Anderson, A.V. Holden, E. Pervolaraki, and F.C. Wen, "Cardiac re-entry dynamics & self-termination in DT-MRI based model of Human Foetal Heart", *Frontiers Phys.* 6:15, 2018

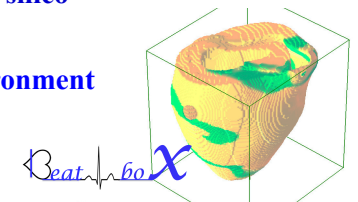
Excitation Re-entry in Rat Pulmonary Vein Wall*



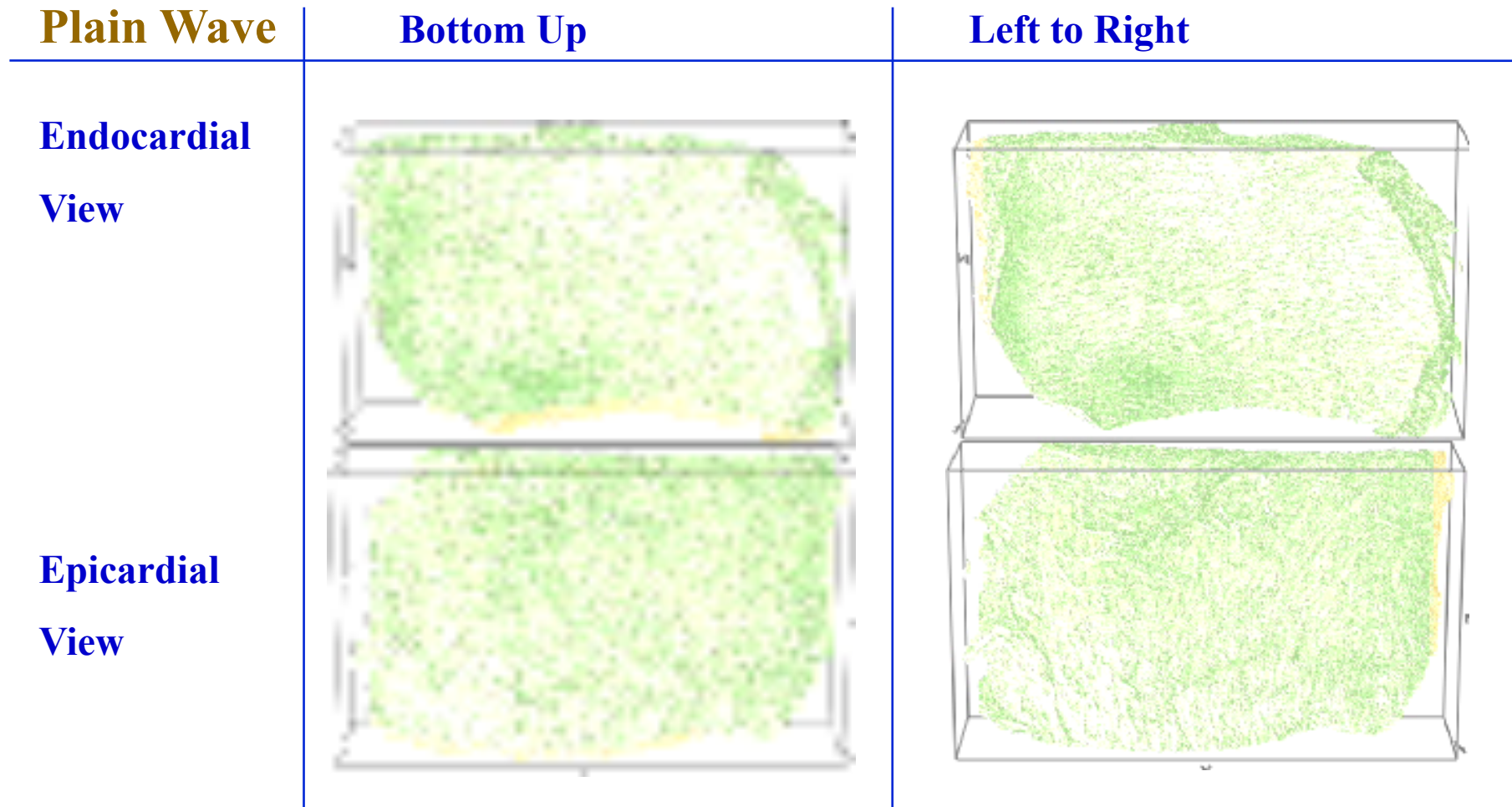
- Regular Cartesian coordinates (micro-CT):
box of $255 \times 920 \times 542$ points, $\Delta x = 3,5 \mu\text{m}$
- Explicit Euler in time
- Second order approximation of Laplacian
- Neumann boundary conditions: $1 < \text{approximation order} \leq 2$ **
- FHN model: $\varepsilon = 0.3$; $\beta = 0.71$; $\gamma = 0.5$ (rigid rotation, positive filament tension)
- Spiral wave initiation by phase distribution
- MPI HPC

*G.S. Ramlugun, B. Thomas, V.N. Biktashev, I.J. LeGrice, B.H. Smaill, J.C. Zhao, and I.V. Biktasheva, "Comparative in-silico study of cardiac re-entry dynamics in micro-CT based models of mammalian hearts", *under review*, 2018.

** M. Antonioletti, V.N. Biktashev, A. Jackson, S.R. Kharche, T. Stary, I.V. Biktasheva, "BeatBox—HPC simulation environment for biophysically and anatomically realistic cardiac electrophysiology". *PLoS ONE* 12(5): e0172292, 2017.



Anatomy Initiated Re-entry in the Rat PV Wall

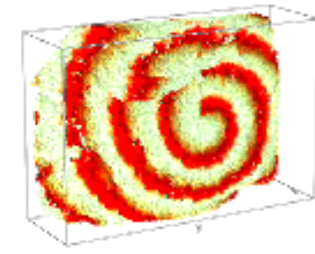
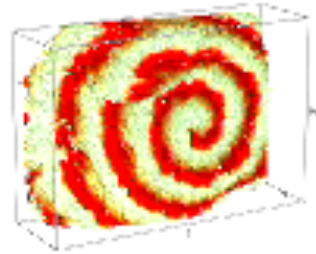


G.S. Ramlugun, B. Thomas, V.N. Biktashev, I.J. LeGrice, B.H. Smail, J.C. Zhao, and I.V. Biktasheva, "Comparative in-silico study of cardiac re-entry dynamics in micro-CT based models of mammalian hearts", *under review*, 2018.

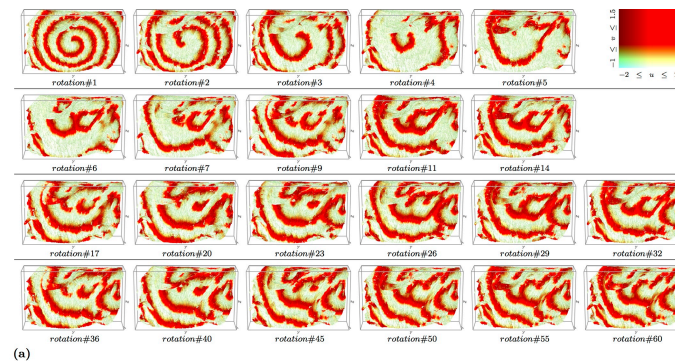
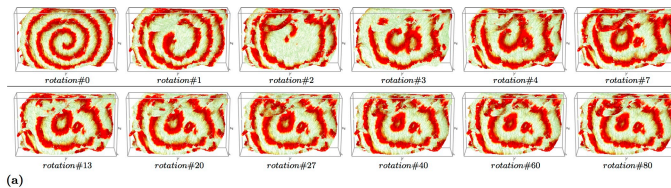
Excitation Re-entry in Rat Pulmonary Vein Wall

Clockwise

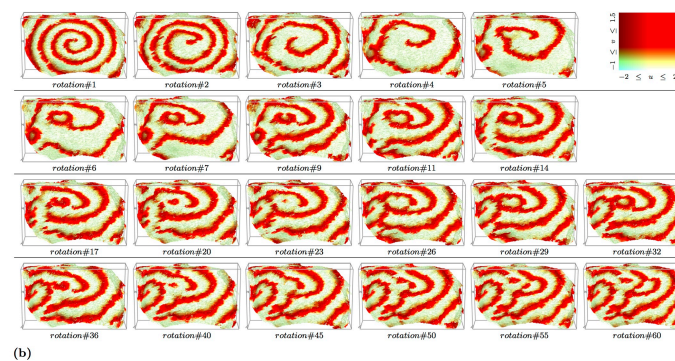
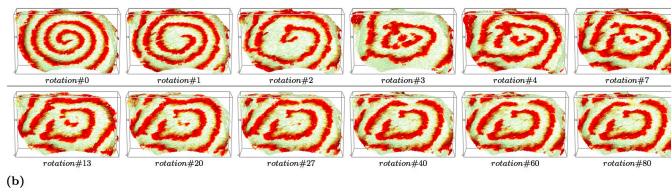
Counter Clockwise



Epicardial View

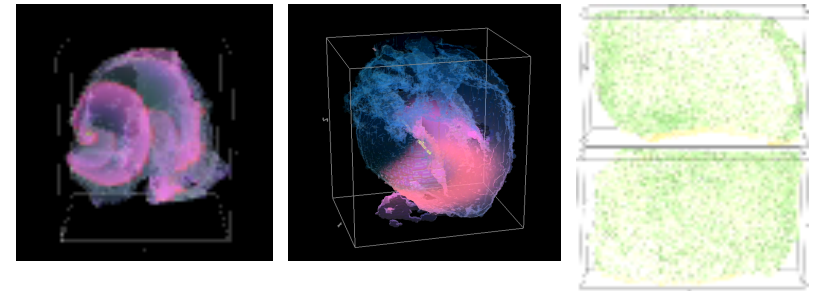


Endocardial View



G.S. Ramlugun, B. Thomas, V.N. Biktashev, I.J. LeGrice, B.H. Smaill, J.C. Zhao, and I.V. Biktasheva, "Comparative in-silico study of cardiac re-entry dynamics in micro-CT based models of mammalian hearts", *under review*, 2018.

Conclusion

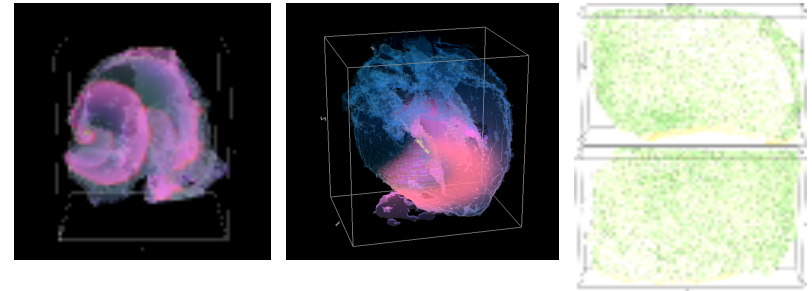


- **DT-MRI/micro-CT models** allow in-silico testing of the effects of individual heart anatomy and anisotropy on cardiac re-entry dynamics.
- **Major Limitation: only “tissue”/“not tissue” points differentiation taken into account.** Currently, tissue segmentation is acquired from DT-MRI data sets via image post-processing. In the future, multichannel computer tomography might offer automatic tissue segmentation.
- **Minor Limitation: challenging visualization** – further research necessary.
- The DT-MRI/micro-CT based comparative study suggests **cardiac anatomy and anisotropy functional effect on cardiac re-entry**: normally self-termination due to the structured shape and anisotropy of the heart; occasionally transition to anatomical re-entry as well as pinning to fine anatomical features.
- In particular, the anatomically realistic cardiac re-entry simulations concur with propensity to pin to PM-CT junction reported in experiment:
 - T. J. Wu, et al., *Circulation Research* 83, 448 (1998).
 - M. Yamazaki, et al., *Cardiovascular Research* 94, 48 (2012).
- Anatomy defined initiation of re-entry.
- Possibility of different endo- vs epi cardial manifestation of trans mural PV wall re-entry.
- Important implications for cardiac re-entry control, e.g. ablation, ICDs, etc.

Acknowledgements:

This work was supported by

- EPSRC, UK (EP/D074789/1, EP/I029664/1): VNB, IVB.
- MRC, UK (G1100357): RAA.
- EPSRC, UK (EP/P008690/1): IVB.
- Health Research Council of New Zealand: GR, BS



We are grateful to

- M.Antonioletti, A.Jackson, A.Karpov, and R.McFarlane
(BeatBox)

Software

- **BeatBox**
<http://empslocal.ex.ac.uk/people/staff/vnb262/software/BeatBox/>
- **EZView**
(Barkley and Dowle's EZScroll descendant for visualization
<http://homepages.warwick.ac.uk/~masax/>)